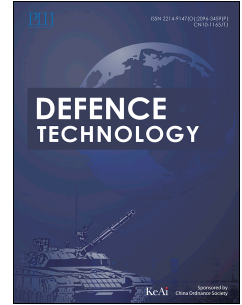


Journal Pre-proof

Ballistic performance of spaced multi-ply soft fabrics: Experimental and numerical investigation

Zhongwei Zhang, Xiaoning Yang, Yuan Lin, Ziming Xiong, Yuhang Xiang, Yi Zhou, Mingyang Wang



PII: S2214-9147(23)00326-4

DOI: <https://doi.org/10.1016/j.dt.2023.12.003>

Reference: DT 1375

To appear in: *Defence Technology*

Received Date: 3 September 2023

Revised Date: 27 October 2023

Accepted Date: 4 December 2023

Please cite this article as: Zhang Z, Yang X, Lin Y, Xiong Z, Xiang Y, Zhou Y, Wang M, Ballistic performance of spaced multi-ply soft fabrics: Experimental and numerical investigation, *Defence Technology* (2024), doi: <https://doi.org/10.1016/j.dt.2023.12.003>.

This is a PDF file of an article that has undergone enhancements after acceptance, such as the addition of a cover page and metadata, and formatting for readability, but it is not yet the definitive version of record. This version will undergo additional copyediting, typesetting and review before it is published in its final form, but we are providing this version to give early visibility of the article. Please note that, during the production process, errors may be discovered which could affect the content, and all legal disclaimers that apply to the journal pertain.

© 2023 China Ordnance Society. Publishing services by Elsevier B.V. on behalf of KeAi Communications Co. Ltd.

Ballistic performance of spaced multi-ply soft fabrics: experimental and numerical investigation

Zhongwei Zhang ^{a,*}, Xiaoning Yang ^{a,b}, Yuan Lin ^a, Ziming Xiong ^a, Yuhang Xiang ^{a,b}, Yi Zhou ^{b,c,**},
Mingyang Wang ^a

^a State Key Laboratory of Explosion & Impact and Disaster Prevention & Mitigation, Army Engineering University of PLA, Nanjing 210007, China

^b School of mechanical engineering, Nanjing University of Science & Technology, Nanjing 210007, China

^c State Key Laboratory of New Textile Materials and Advanced Processing Technologies, Wuhan Textile University, Wuhan 430200, China

***Corresponding author:** Zhongwei Zhang

E-mail: zhangzhongwei.cn@gmail.com

****Corresponding author:** Yi Zhou

E-mail: yi.zhou@wtu.edu.cn

Ballistic performance of spaced multi-ply soft fabrics: experimental and numerical investigation

Abstract

It has been reported that the ply gap influences the ballistic resistance of spaced multi-ply fabric systems, but its working mechanism was not well-understood. This paper reports the experimental and numerical approaches and results of an investigation on the mechanisms that enable the improved ballistic performance of spaced multi-ply systems. Penetration tests were performed over a range of impact velocities ranging from 200–400 m/s. The results confirmed that the ply gap is beneficial to the energy absorption capability of the systems. This is because the front plies tend to absorb more energy when they are not immediately constrained by the rear plies. During a ballistic event, the gap relieves the reflection of the compressive pulse, prolonging the projectile engagement time with the front plies; on the other hand, the rear plies become increasingly less active in dissipating energy as the gap increases. When the gap is sufficiently widened to avoid any interference between the plies before the failure of the front ply, the responses of the whole system no longer vary. It was also found that the ballistic performance of the spaced systems is influenced by ply thickness, impact velocity, and the stacking order of the ply gap.

Keywords: Energy absorption capability; Ply gap; Ballistic performance; The front ply; The rear ply

Ballistic performance of spaced multi-ply soft fabrics: experimental and numerical investigation

Abstract

It has been reported that the ply gap influences the ballistic resistance of spaced multi-ply fabric systems, but its working mechanism was not well-understood. This paper reports the experimental and numerical approaches and results of an investigation on the mechanisms that enable the improved ballistic performance of spaced multi-ply systems. Penetration tests were performed over a range of impact velocities ranging from 200–400 m/s. The results confirmed that the ply gap is beneficial to the energy absorption capability of the systems. This is because the front plies tend to absorb more energy when they are not immediately constrained by the rear plies. During a ballistic event, the gap relieves the reflection of the compressive pulse, prolonging the projectile engagement time with the front plies; on the other hand, the rear plies become increasingly less active in dissipating energy as the gap increases. When the gap is sufficiently widened to avoid any interference between the plies before the failure of the front ply, the responses of the whole system no longer vary. It was also found that the ballistic performance of the spaced systems is influenced by ply thickness, impact velocity, and the stacking order of the ply gap.

Keywords: Energy absorption capability; Ply gap; Ballistic performance; The front ply; The rear ply

1. Introduction

Modern soft armors used in ballistic impact protection systems consist of many layers of flexible materials, and it offers protection by absorbing and dissipating projectile kinetic energy, showing enormous potential for energy absorption in the ballistic events [1–4]. It has been widely accepted that while fiber properties play an essential role in determining the energy absorption capability subjected to ballistic events, the influence of structural effect is non-negligible. The structural impact includes, but is not limited to, yarn structure, fabric pattern, and panel constituent, among which the interference between the neighboring plies in a flexible ballistic panel attracted much attention [5–6].

Some researchers believe that enhancing the interference between the adjacent plies is desirable for energy absorption. Porwal and Phoenix [7] developed an analytical model to study the influence of varying the ply gap on panel performance. They found that the V_{50} , velocity of the projectile at which there is a 50% probability of perforating the target material, decreases as the gaps between the adjacent plies increase. Eliminating gaps between plies and hence enhancing ply coupling is beneficial to performance improvement. Ply coupling can be further improved by varying ply orientations. Wang et al. [8–9] demonstrated the benefit of designing angle-ply panels in their experimental and numerical investigation of multi-ply fabric systems. A 14% increase in energy absorption was found in angled fabric panels compared with aligned fabric panels. Liu et al. [10] investigated the ballistic performance of helicoidal laminates, indicating that the mixed configuration composed by both helicoidal and cross-ply laminates outperformed quasi-isotropic laminates by 86.6% in terms of impact energy absorbed. They also found that the perforation energy of CFRP laminates can be significantly improved by optimizing ply blocking configuration, achieving a maximum increase of 64% in perforation energy [11]. An increase of 58% was found by Arora et al. [12] in their investigation of treating angle-ply fabric panels with shear thickening fluid (STF). They attributed the improvement to the propagation of stress waves in multiple directions and the engagement of more secondary yarns in an angle-ply fabric panel during a ballistic performance. Yuan et al. [13] found that angle-ply panels had approximately 10% larger stressed areas in the first and middle plies than those of aligned panels.

Nevertheless, investigations into the ballistic performance of cross-ply ultra-high-molecular-weight polyethylene laminates showed that angle-ply panels exhibit inferior performance than aligned panels [14–15], and therefore some researchers pointed out that ply coupling is detrimental to the energy absorption capability of a multi-ply fabric system. Cunniff [16] suggested that the subsequent plies transfer the stress back to the first few plies, resulting in stress concentration and earlier failure at the impact point. In addition, adding subsequent plies constrains the transverse deflection of the first plies, amplifies stress concentration, and reduces the amount of energy absorbed by the material. This suggestion corroborates the findings of Zhou et al. [17] and Chen et al. [18]. They used finite element (FE) models to predict the performance of multi-ply woven fabric systems. Cunniff [16] tested

a double-ply system consisting of Kevlar 29 and Spectra 1000 woven fabric and pointed out that placing low modulus material on the impact face and high modulus material on the back face eliminates the contact between plies and therefore creates higher V_{50} . The experimental observation was confirmed by Porwal and Phoenix [19] in their work of using a computational model to investigate the effects of stacking sequences of fabric plies. They also suggested that if severe thermal softening of Spectra ply was not considered, the differences in V_{50} for the two possible arrangements would be much smaller than those observed in Cunniff's work. Zhou et al. [20] used a FE model to simulate the ballistic event and found that Dyneema/Kevlar system exhibits 16% less energy absorption than the reversed sequence. The interference between plies was believed to be the main contributor to inferior performance. Lim et al. [21] used different projectiles to test the performance of spaced and non-spaced double-ply fabric systems. They found that spaced systems perform better than non-spaced systems when impacted by flat-nose and hemispherical projectiles. Spaced systems exhibit inferior performance when impacted by ogival and conical projectiles.

While there are a number of articles in the literature on the ballistic impact responses of multi-ply woven fabric systems, little work has been done to characterize the effects of the ply gap on panel performance, especially the responses and energy absorption mechanisms of the front and rear plies upon ballistic impact. In this paper, both ballistic penetration tests and FE simulation will be used to comprehensively study the performance and identify the underlying energy absorption mechanisms of spaced multi-ply fabric systems. The influence of the ply gap, system thickness, impact velocity, and stacking order of the ply gap will be investigated. The optimum architecture will be developed for the engineering design of lightweight, flexible fortification system or anti-ballistic tent.

2. Material and panel specification

Plain weave fabrics were manufactured from Kevlar®29 multi-filament yarns. The fabrics have a yarn linear density of 1670 dtex and a thread density of 7.25 threads/cm. The areal density of the fabrics is 240 g/m². Ethylene-vinyl acetate copolymer (EVA) foam was used as spacing material to control the width of the ply gap in multi-ply systems since the penetration testing results showed that the EVA foam does not exhibit any ballistic performance. The mechanical properties of Kevlar®29 multi-filament yarn and EVA in use are shown in Table 1.

Table 1
Material specifications.

	Kevlar®29	EVA foam
Material	Aramid	Ethylene-vinyl acetate copolymer
Yarn type	Multi-filament yarn	-
Breaking strength/MPa	2920	0.12
Breaking elongation/%	3.6	90
Modulus/MPa	70500	1.03
Yarn count/dtex	1670	-
Density/(kg·m ⁻³)	1440	18

Four influencing factors will be studied: the ply gap, system thickness, impact velocity, and stacking order of the ply gap. The panels were designed in such a way that half of the plies were placed near the impact face, and half of the plies were placed away from the impact face, i.e., "2+2" for a four-ply system and "3+3" for six-ply systems, the combinations of which are shown in Table 2. Ply gap is normalized by ply thickness, which refers to G . The value of G can be obtained from the following equation:

$$G = D_{\text{gap}} / T_{\text{fp}} \quad (1)$$

where D_{gap} is the gap distance between the front and rear sets of ply, T_{fp} is the thickness of the front ply/plies. For example, the thickness of a single-ply fabric is 0.4 mm, and a spaced "1+1" system with a ply gap of 1 mm indicates that $G=2.5$. In terms of spaced systems of "2+2" and "3+3", T_{fp} is the thickness of the front set of plies. A spaced "2+2" system with a gap distance of 2 mm also has a $G=2.5$, as the front set contains two plies and the value of T_{fp} is 0.8 mm. A spaced "3+3" system with a gap distance of 6 mm has a $G=5$, as the front set contains three plies and the value of T_{fp} is 1.2 mm.

These combinations will be tested at an impact velocity of 400 m/s. In addition, the "1+1" systems are subjected to ballistic penetration at the impact velocities of 200 m/s (40 J), 283 m/s (80 J), 346 m/s (120 J), and 400 m/s (160 J). The responses will be analyzed by numerical prediction. In the end, two types of panels were designed (Type A & Type B) to study the stacking order of the ply gap. The tests were performed at an impact velocity of approximately 400 m/s. In Type A panels, the system consists of six plies of woven fabrics, and some of the fabric plies were

separated into three sets with different locations with a ply gap. In type B panels, the system consists of three plies of woven fabrics. Panel details are given in Table 3.

Table 2

Schematic illustrations of the non-spaced & spaced systems with normalized gap.

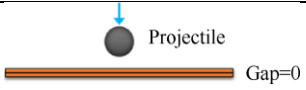
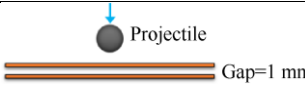
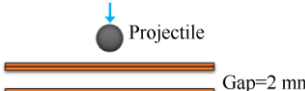
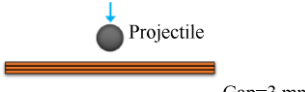
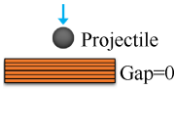
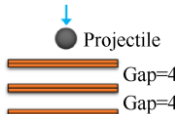
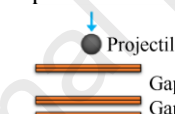
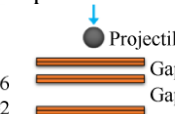
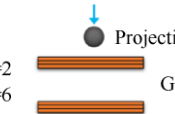
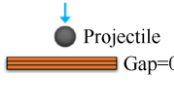
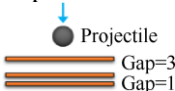
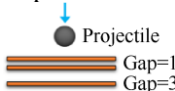
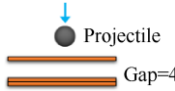
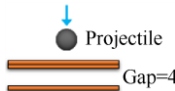
Multi-ply systems	$G = 0$	$G = 2.5$	$G = 5$
1+1			
2+2			
3+3			

Table 3

Details of Type A & Type B panels with different stacking order of the ply gap.

Type A1	Type A2	Type A3	Type A4	Type A5	
6 plies without ply gap	2 plies+4 mm+2 plies +4 mm+2 plies	2 plies+6 mm+2 plies +2 mm+2 plies	2 plies+2 mm+2 plies +6 mm+2 plies	3 plies+8 mm+3 plies	
					
Type B1	Type B2	Type B3	Type B4	Type B5	Type B6
3 plies without ply gap	1 plies+2 mm+1 plies +2 mm+1 plies	1 plies+3 mm+1 plies +1 mm+1 plies	1 plies+1 mm+1 plies +3 mm+1 plies	1 plies+4 mm+2 plies	2 plies+4 mm+2 plies
					

3. Ballistic impact test

This section describes how the ballistic penetration tests were performed. The ballistic impact tests were performed on a set-up shown in Fig. 1. The method used for the measurements was detailed in previous Ref. [22], and a brief description will be given in this paper. In this ballistic apparatus, the spherical steel projectile in use is 2 grams in weight and 8 mm in diameter. The projectile is propelled by high-pressure nitrogen and accelerated in a launch tube. The impact velocity varies in the range of 200–400 m/s. Sabot made of Polycarbonate was used to propel the projectile, which is shown in Fig. 1(a). The sabot is removed by a shelling device at the end of the barrel. The penetration tests were performed in a chamber made of armor plate. The recycling device is made of armor rubber. An edge-clamped fixture was designed to clamp the sample target in the ballistic impact test, as displayed in Fig. 2(a). In this fixture, the Multi-ply fabric was gripped at its four edges to avoid yarn pull-out during the ballistic impact event. The area exposed to impact is 15 cm×15 cm. Fixing bolts were through-bolted with the backplate and fastened by screw nuts. The bolt in use is 10 mm in diameter and 60 mm in length. The torque is 280 N·m. The slipping of the fabric is avoided by the ridges and grooves in the inner surface of the fixtures. Additional G clamps were used on the edges for thick panels. Samples were tailored to fit the sample size shown in Fig. 1(b). Each sample was tested three times. The Kevlar fabrics and foam are stacked together rather than glued together. A Photron FASTCAM SA-Z high-speed camera was used to measure the

impact and the residual velocities of the projectile. Fig. 1(c) shows the trajectory of a projectile before and after fabric penetration. The images were recorded at a frame rate of 20000 fps, a resolution of 512 px × 512 px, and an exposure time of 8.8 μs. The velocity can then be obtained by identifying the distance between the adjacent projectiles. The energy loss of the projectile can be determined by

$$\Delta E = \frac{1}{2} m (v_1^2 - v_2^2) \quad (2)$$

where ΔE is the kinetic energy loss of the projectile, m is the mass of the projectile, and v_1 and v_2 are impact and residual velocities of the projectile, respectively. In this research, the effect of air drag on the projectile was considered a vital factor of projectile kinetic energy loss, and the energy dissipated by air drag increases exponentially with the impact velocity. The energy dissipated by air drag can be measured by shooting a projectile without fixing the sample target on the clamp. By removing this portion of energy loss ΔE , energy absorbed by the sample target can be calculated. This value was used as an indicator of its ballistic performance.

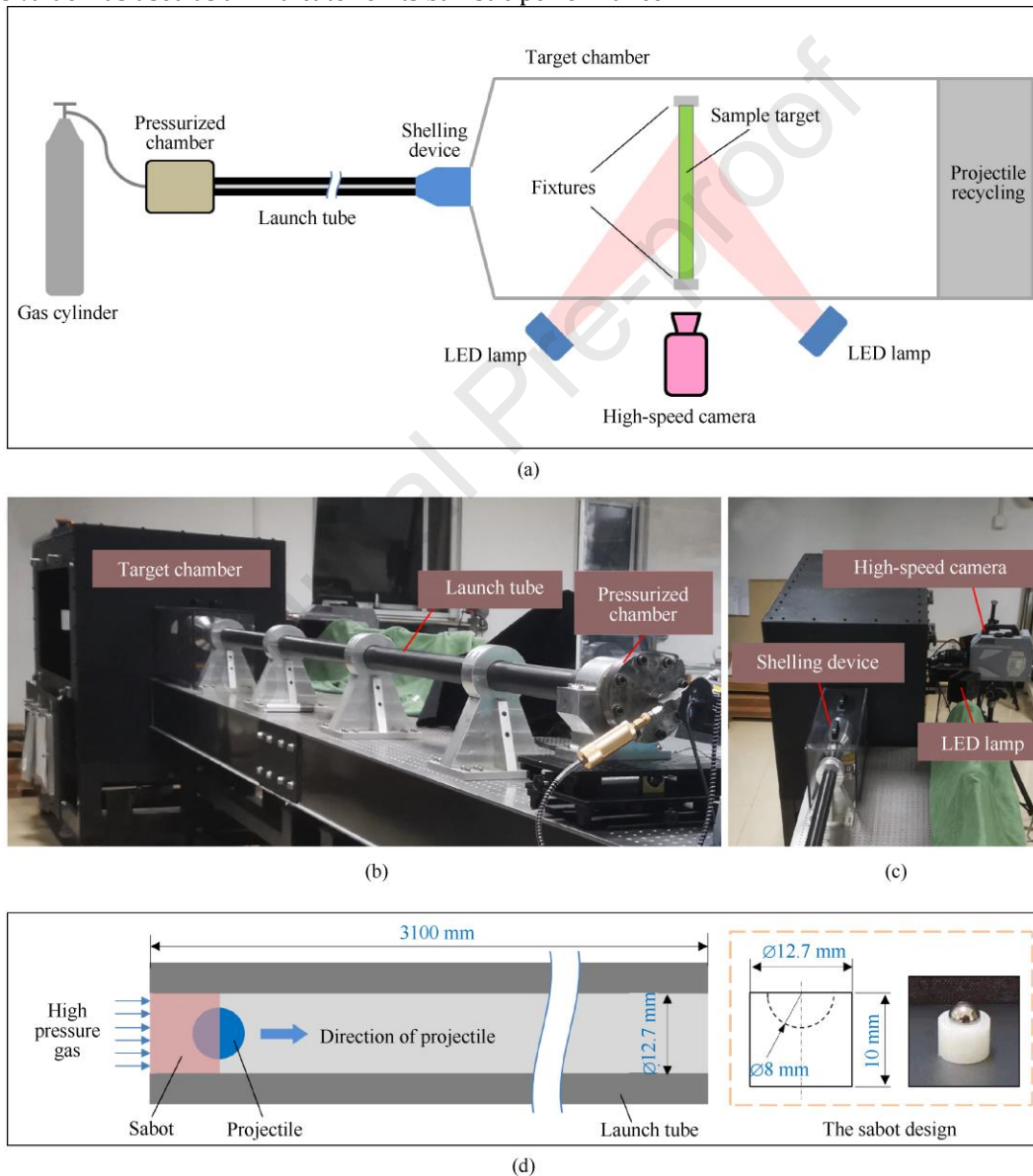


Fig. 1. The ballistic impact testing system: (a) Schematic of the ballistic impact testing; (b) Side view of the experimental devices; (c) Top view of the experimental devices; (d) The design of sabot and launch tube.

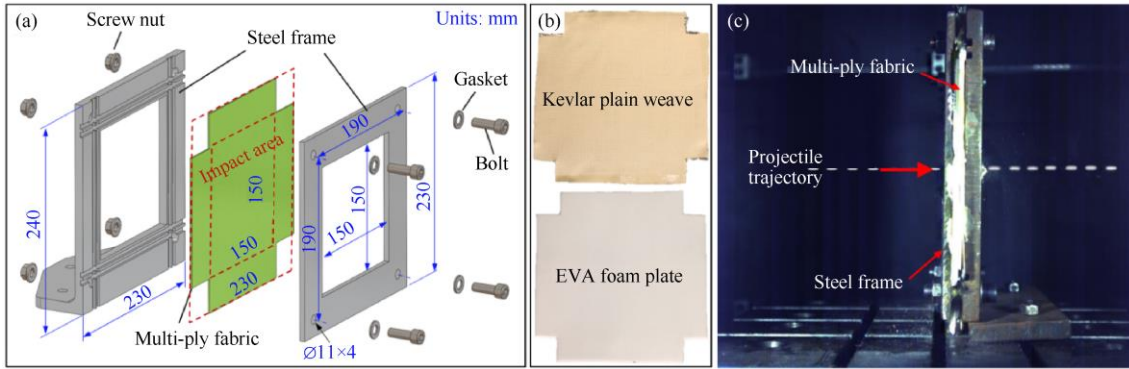


Fig. 2. The edge-clamped fixture: (a) Schematic diagram; (b) Tailored samples; (c) Velocity capture.

4. FE simulation

4.1. Geometry model

The solver ABAQUS® 2020 Explicit was used to simulate the ballistic impact, enabling the investigation of the fabric deformation, stress distribution, and energy absorption evolution during the ballistic event. In this research, FE simulation is limited to colliding between a projectile of rigid material and flexible single-ply fabrics. The projectile model is spherical, with the diameter being 8 mm, and the mass of the projectile being 2 grams, identical to the one used for practical ballistic tests. Fabrics were simulated at the yarn level to capture displacement during a ballistic event. The yarn was modeled as 3D solid geometry with undulated crimps and lenticular cross-sections according to their corresponding yarn geometry (Fig. 3(a)). In order to make the model less computationally expensive, a hybrid meshing scheme was adopted. For the primary yarns, mesh density was adopted with six elements in one yarn cross-section and twelve elements in one yarn wavelength (Fig. 3(b)). The mesh size is 0.18 mm. For the secondary yarns, four and eight elements were involved in one yarn cross-section and wavelength, respectively (Fig. 3(c)). The mesh size is 0.4 mm. This technique has been proved to provide sufficient accuracy for multi-ply system modeling while the computational resource is limited [23–25]. Eight node hexahedron elements (C3D8R) were used for yarns and the projectile in the model. Yarns were assembled in the warp and weft directions to construct a plain weave of 150 mm×150 mm, and fixed boundary conditions (six degrees of freedom have been constrained) were assigned for the fabric edges. Symmetric boundary conditions about the X and Z axes were applied to the other two edges to save computational resources. Therefore, the amount of energy absorbed by the fabrics obtained from the FE simulation was multiplied by a factor of four to compare the experimental results.

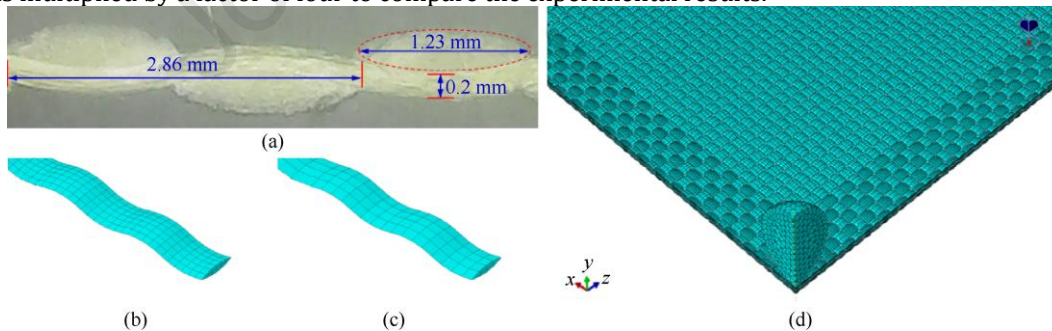


Fig. 3. The meshing of FE models for a “1+1” fabric system: (a) The cross-section of the plain weave; (b) Fine mesh in a primary yarn; (c) Coarse mesh in a secondary yarn; (d) Hybrid mesh in the fabric model.

4.2. Material

Yarns were modeled as homogenous continua to represent the filament-level architecture. The material is assumed to be orthotropic, with a linear elastic relation between stress and strain described as

$$\begin{bmatrix} \varepsilon_{xx} \\ \varepsilon_{yy} \\ \varepsilon_{zz} \\ \gamma_{yz} \\ \gamma_{zx} \\ \gamma_{xy} \end{bmatrix} = \begin{bmatrix} \frac{1}{E_{xx}} & -\frac{\nu_{xy}}{E_{yy}} & -\frac{\nu_{xz}}{E_{zz}} & 0 & 0 & 0 \\ -\frac{\nu_{yx}}{E_{xx}} & \frac{1}{E_{yy}} & -\frac{\nu_{yz}}{E_{zz}} & 0 & 0 & 0 \\ -\frac{\nu_{zx}}{E_{xx}} & -\frac{\nu_{zy}}{E_{yy}} & \frac{1}{E_{zz}} & 0 & 0 & 0 \\ 0 & 0 & 0 & \frac{1}{G_{yz}} & 0 & 0 \\ 0 & 0 & 0 & 0 & \frac{1}{G_{zx}} & 0 \\ 0 & 0 & 0 & 0 & 0 & \frac{1}{G_{xy}} \end{bmatrix} \begin{bmatrix} \sigma_{xx} \\ \sigma_{yy} \\ \sigma_{zz} \\ \tau_{yz} \\ \tau_{zx} \\ \tau_{xy} \end{bmatrix}$$

where the E , G and ν were the elastic modulus, shear modulus, and Poisson's ratio. E_{xx} is the modulus of the material along the yarn direction, which is assumed to be equal to 70.5 GPa. The values of E_{yy} and E_{zz} (GPa) are obtained from Ref. [26]. The values of shear modulus and Poisson's value are cited from Refs. [26–27].

The damage onset criterion in use is a phenomenological model for predicting the onset of damage due to nucleation, growth, and coalescence of voids within the material. The model assumes that the criterion for damage initiation is met when the following condition is satisfied

$$\omega_D = \int \frac{d\bar{\varepsilon}^{pl}}{\bar{\varepsilon}_0^{pl}} = 1 \quad (3)$$

where ω_D is a state variable that increases monotonically with plastic deformation, $\bar{\varepsilon}^{pl}$ is the equivalent plastic strain, $\bar{\varepsilon}_0^{pl}$ is the equivalent plastic strain at the onset of damage. At each increment during the analysis the incremental increase in ω_D is computed as

$$\omega_D = \frac{\Delta\bar{\varepsilon}^{pl}}{\bar{\varepsilon}_0^{pl}} \geq 0 \quad (4)$$

As the material is linear elastic and has limited plastic deformation, a yield stress (σ_{y0}) of 2.92 GPa and equivalent plastic strain at the onset of damage ($\bar{\varepsilon}_0^{pl}$) of 0 were set for the model. That means the material has no plastic deformation and damage is initiated immediately when the stress of the element reaches 2.92 GPa. When material damage occurs, the stress-strain relationship no longer accurately represents the material's behavior. Continuing to use the stress-strain relation introduces a strong mesh dependency based on strain localization, such that the energy dissipated decreases as the mesh is refined. A different approach is required to follow the strain-softening branch of the stress-strain response curve. Hillerborg's fracture energy proposal is used to reduce mesh dependency by creating a stress-displacement response after damage is initiated. Using brittle fracture concepts, Hillerborg [28] defines the energy required to open a unit area of crack, G_f , as a material parameter. With this approach, the softening response after damage initiation is characterized by a stress-displacement response rather than a stress-strain response.

The implementation of this stress-displacement concept in a finite element model requires the definition of equivalent plastic displacement, $\bar{u}^{pl} = L\bar{\varepsilon}^{pl}$. L is a characteristic length that depends on the element geometry and formulation. When damage evolution is based on energy dissipated during the damage process, we can specify the fracture energy per unit area, G_f , to be dissipated during the damage process directly. The exponential evolution process is defined by:

$$d = 1 - \exp\left(-\int_0^{\bar{u}^{pl}} \frac{\sigma_y d\bar{u}^{pl}}{G_f}\right) \quad (5)$$

where d is damage variable which increases progressively with \bar{u}^{pl} . The formulation of the model ensures that the energy dissipated during the damage evolution process is equal to G_f , as shown in the following figure. In theory, when the damage variable, d , reaches 1, damage evolution process is completed. In practice, Abaqus/Explicit will set d equal to 1 when the dissipated energy reaches a value of $0.99G_f$. Therefore, the fracture energy G_f is the energy required to open a unit area of crack. With this parameter, the softening response after damage initiation can be characterized by a stress-displacement response. Our preliminary work showed that the value of fracture energy has limited influence on the energy absorption capability of the material. Nevertheless, a value is needed to identify the process of fracture evolution. In addition, G_f can be expressed by:

$$G_f = \int_0^{\bar{u}^{pl}} \sigma_y d\bar{u}^{pl} \quad (6)$$

the value of fracture energy per unit area was set to 500 J [1, 22, 29].

The projectile was modeled as a rigid body and was not deformed during the impacting process. The material properties are listed in Table 2. A general contact interaction was used to define the contact between the projectile and the sample target and between the interlaced warp and weft yarns. For general contact Abaqus/Explicit enforces contact constraints using a penalty contact method, which searches for node-into-face and edge-into-edge penetrations in the current configuration. The penalty stiffness that relates the contact force to the penetration distance is chosen automatically by Abaqus/Explicit so that the effect on the time increment is minimal, yet the penetration is not significant. The coefficient of friction, μ , was set to 0.22 [30]. The EVA foam was not modeled in the simulation because it provides limited resistance against ballistic impact. The calculation time depends on the impact velocity of the projectile, i.e., in the cases of impact velocity =400 m/s, the calculation time is 50 μ s, in the cases of impact velocity =200 m/s, the calculation time is 100 μ s.

Table 4

Material properties.

Material properties	Projectile	Yarn
E_{xx} /GPa	—	70.5
E_{yy} and E_{zz} /GPa	—	1.34 [26]
G_{xy} and G_{xz} /GPa	—	3.28 [27]
G_{yz} /GPa	—	0.504 [27]
ν_{xy} , ν_{yz} , and ν_{xy}	—	0.2 [26]
Mass density ρ /($\text{kg}\cdot\text{m}^{-3}$)	7800	1440
σ_y /GPa	—	2.92
$\bar{\epsilon}_o^{\text{pl}}$	—	0
G_f	—	500 [1, 22, 29]
μ	0.22	0.22 [30]

4.3. Model validation

The FE model was validated by simulating the ballistic impact at different impact velocities and by comparing the deformation of the numerical model with images obtained from the high-speed camera. Fig. 4 compares the FE and experimental results for the variation of residual velocity as a function of the impact velocity for two-, four- and six-layer non-spaced fabric systems. A close resemblance was found between the FE and experimental results. The numerical predictions show that the ballistic limits of the three above fabric systems are approximately 119 m/s, 194 m/s, and 239 m/s, respectively. The non-linear and linear increasing trend of the curves beyond the ballistic limit can be explained by the transition from the elastic response of the fabrics to the inelastic response of the fabrics as the impact velocity increases [31]. Fig. 5 shows the fabric deformation of a double-ply fabric system and FE predictions at an impact velocity of 400 m/s. A full size model was used to present the deformation so that the numerical predictions can be compared with the images from the high-speed photography. It must be noted here that the numerical data displayed in section 5 was still obtained from quarter models. Both high-speed images and the FE model exhibit the pyramid-like transverse deflections, and the marker of yarn de-crimping was also noticed on the fabric surface.

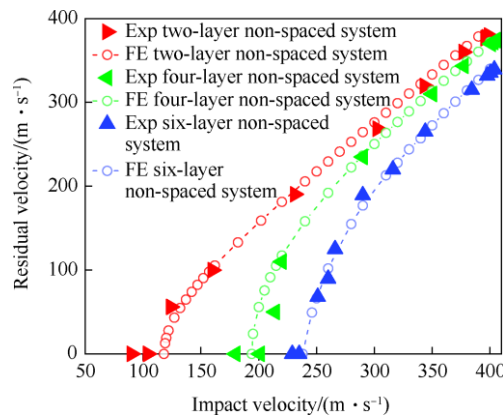


Fig. 4. Comparison of FE and experimental results of the multi-ply fabric systems.

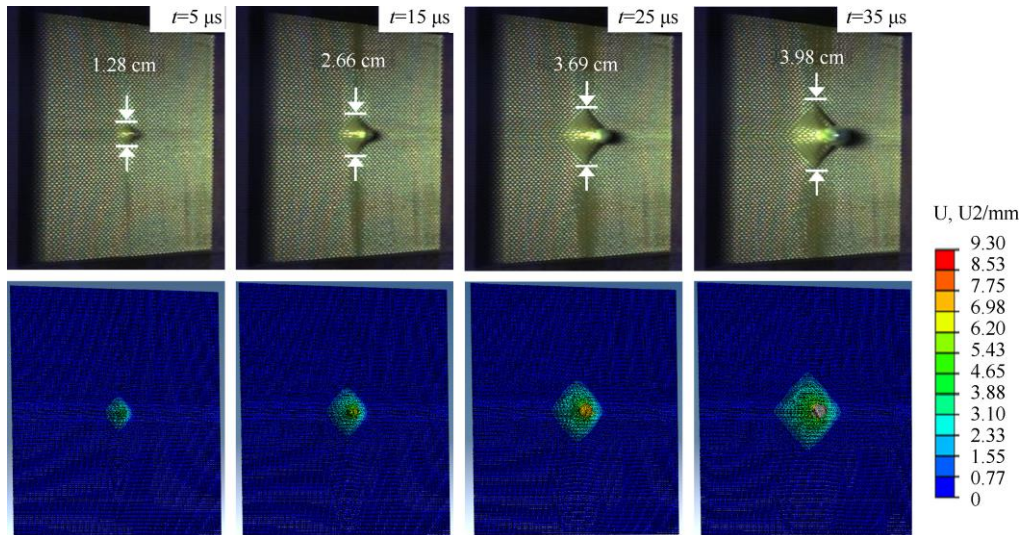


Fig. 5. High-speed images and FE simulation of a double-ply fabric system at an impact velocity of 400 m/s.

4.4. Characterization of fabric responses

The responses of the front and rear sets of plies were characterized by the projectile-fabric engagement time and the amount of energy absorbed. Hence, it is important to find out the breakage time of the corresponding set of plies. Fig. 6 shows the time history of the strain and kinetic energy of a non-spaced double-ply system. During a ballistic event, the loading of the impacting projectile causes the energy evolution curves to exhibit a peak. As the peaks of the strain energy curve seem to occur way beyond fabric penetration, which is identifiably clear in Fig. 6, the peaks of the kinetic energy curve appear to be a more reasonable indicator of fabric breakage time. It follows that the projectile-fabric engagement time can be determined by the duration between the initiation and the peak of the kinetic energy curve. As it is difficult to quantify the amount of frictional energy absorbed by the constituent layers, the amount of energy absorbed is determined to be the sum of the kinetic and strain energy at breakage. Fig. 6 shows the energy evolution history of the front and rear plies in a “1+1” system (Seen in Table 2). In terms of “2+2” and “3+3” systems, both the front plies and rear plies were considered as a whole in FE simulation to make the numerical analysis more tractable. The interaction behavior between the front and rear sets of plies will be analyzed in this research. The interaction time is determined to be the duration between the onset of the kinetic energy curve of ply two and the peak point of that of ply one. In Fig. 6, the duration of interaction is 9.8 μ s. When there is a gap in the system, the response of the rear plies will be delayed.

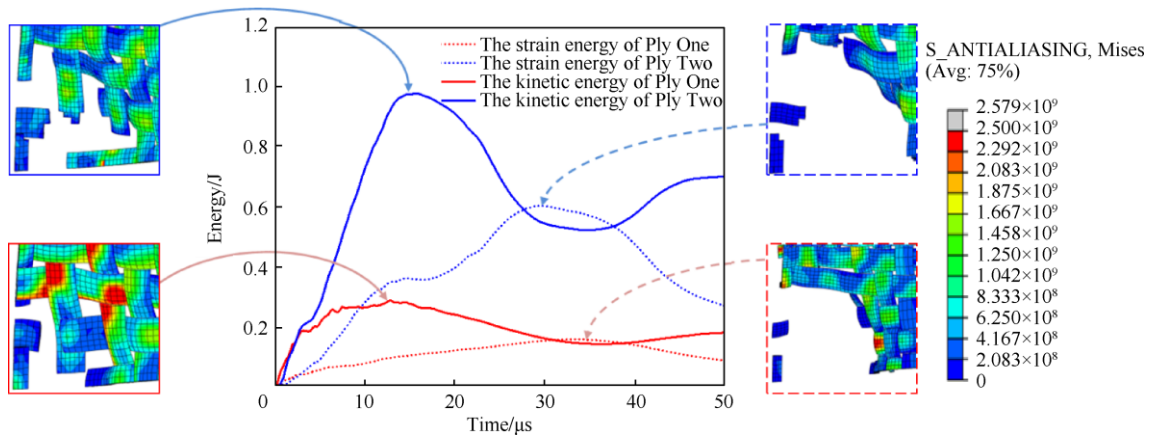


Fig. 6. Energy evolution of the nonspaced double-ply system at an impact velocity of 400 m/s.

5. Results and discussion

In this section, “1+1”, “2+2”, and “3+3” fabric systems shown in Table 2 were selected to study the underlying energy absorption mechanism of spaced systems upon ballistic impact. Fig. 7

displays the plot of energy absorption against normalized gap G . Research was undertaken on systems with normalized gaps G up to 10. This is convenient to achieve in FE simulation. In ballistic shooting test, the value of G for system “1+1” is 0 (Gap=0 mm), 2.5(Gap=1 mm), 5(Gap=2 mm), 7.5(Gap=3 mm) and 10(Gap=4 mm); the value of G for system “2+2” is 0 (Gap=0 mm), 2.5(Gap=2 mm), 5(Gap=4 mm), 7.5(Gap=6 mm) and 10(Gap=8 mm); the value of G for system “3+3” is 0(Gap=0 mm), 1.67(Gap=0 mm), 3.34(Gap=4 mm), 5(Gap=6 mm) and 6.67(Gap=8 mm). When the value of G is greater than 6.67 (Gap=12 mm) for system “3+3”, it is very difficult for the clamp to constrain the fabric edge tightly. Yarn tails tend to slip from the clamp, and therefore, the ballistic results would be biased. The amount of energy absorbed by the fabrics obtained from the FE simulation was multiplied by a factor of four to compare the experimental results. In Fig. 7, the experimental results were found to be greater than the numerical predictions in thinner systems. The difference becomes less pronounced as the number of ply increases. The amount of energy absorbed by the systems increases almost linearly with the number of plies. In terms of the experimental results, the energy absorption of all the systems increases from $G=0$, reaches a peak and then levels off from that point onwards. The normalized ply gap that provides the first peak energy absorption refers to critical G . The value of critical G appears to range from 2 to 5 for different panels. Take “1+1” systems for instance, a spaced system with $G=5$ absorbs approximately 34.4% more energy than the non-spaced system. The increases in energy absorption at $G=5$ in the optimum spaced panels are 23.7% and 24.2% for “2+2” and “3+3” systems, respectively. Since the EVA foam does not provide impact resistance, the improvement in ballistic performance can only be attributed to the ply gap. The results raise two important questions: why a critical G is there, and why the value of critical G varies with the thickness of the system. These two questions will be further explored in subsections 5.1 and 5.2, respectively.

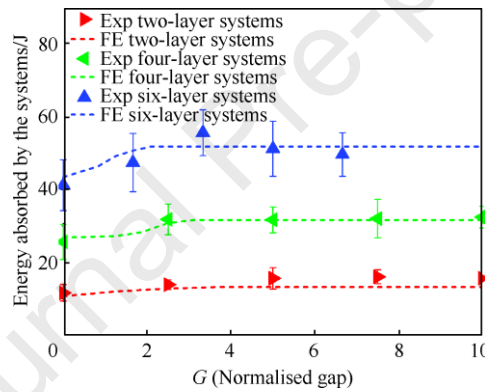


Fig. 7. Comparison of FE and experimental results of multi-ply systems at various ply gaps at an impact velocity of approximately 400 m/s.

5.1. The influence of ply gap

This subsection will study the underlying working mechanisms of the ply gap to elucidate the becoming of critical G . In order to solve this problem, FE simulation was used to analyze fabric deformation, stress distribution, and energy absorption of the “1+1” systems using the method described in subsection 4.4. Three cases, $G=0$, 2.5, and 5, were selected for investigation at the impact velocity of 400 m/s.

During the penetration process, the front and rear plies interact with each other. The duration of interaction, which has been defined in subsection 4.4, is compared in Fig. 8. It was found that the interaction time decreases slightly as the ply gap increases, from 9.8 μ s in the case of $G=0$ to 8 μ s in the case of $G=5$, and the total projectile-fabric engagement time (Fig. 8(a)) and the total amount of energy absorbed (Fig. 8(b)) also increases accordingly, indicating that ply interaction is detrimental to panel performance. In terms of the front ply, fabric breakage time is delayed when the gap increases (Fig. 8(a)). This is because when there is no gap designed for the system, the deformation of the front ply is constrained by the rear ply. The compressive shock wave generated by the impact is reflected from the rear ply as a compressive pulse at the impact site of the front ply [30]. As a result, stress concentration occurs at the impact site, and the material fails at an early stage. When the projectile impacts a spaced system, the gap relieves the reflection of the compressive pulse, and therefore the projectile-fabric engagement time is prolonged. This consequently leads to a slightly more defined transverse deflection and a noticeably larger area of stress distribution in Fig. 9. A more detailed comparison was made in Fig. 10, where the primary yarns of the front and rear plies were extracted from Fig. 9. It is not difficult to find that stress is more concentrated on the front ply

yarn of $G=0$ than those of $G=2.5$ and 5 prior to failure. At $6\text{th } \mu\text{s}$ after impact, the yarn of the unspaced system fails due to the constraint of the rear ply. Accordingly, the amount of strain and kinetic energy absorbed by the front ply increases from $G=0$ to $G=5$ in Fig. 8(b); On the other hand, the rear ply appears to be increasingly less active in energy absorption when G increases, the phenomenon of which was quantified by a decreasing trend of projectile-fabric engagement time in Fig. 8(a) and the sum of strain and kinetic energy absorption in Fig. 8(b). This is because the narrowly spaced systems enable the rear plies to load the projectile at an early stage of the ballistic event and promote more rapid and effective slowing via the absorption of ply strain and kinetic energy after sufficient time has elapsed for penetration. In terms of the widely spaced systems, the response of the rear ply is delayed by the gap and hence becomes less active during the energy absorption process.

By comparing the responses of the front and rear plies, it is not difficult to find that the former is more sensitive to ply gap than the latter, i.e., the variation in projectile-fabric engagement time as well as energy absorption is more dramatic for the front ply than those for the rear ply. For instance, the increase in the projectile-fabric engagement time of the front ply is 23.3% when G increases from 0 to 5 , while the decrease is 8.16% for the rear ply. The variation of stress distribution is more dramatic in the front ply than in the rear ply in Fig. 9. These cause the increase in energy absorption of the former to be greater than the reduction in the energy absorption of the latter. In addition, the projectile-fabric engagement time of the front and rear plies differs by more than 30% when $G=0$ and by less than 10% when $G=5$. It, therefore, appears that increasing the ply gap facilitates assimilating the responses of the front and rear plies, during the process of which the failure of the front ply is delayed, and the amount of energy absorbed by the whole system increases with G up to a critical value beyond which the front and rear plies do not interfere with each other, and their responses cease to vary.

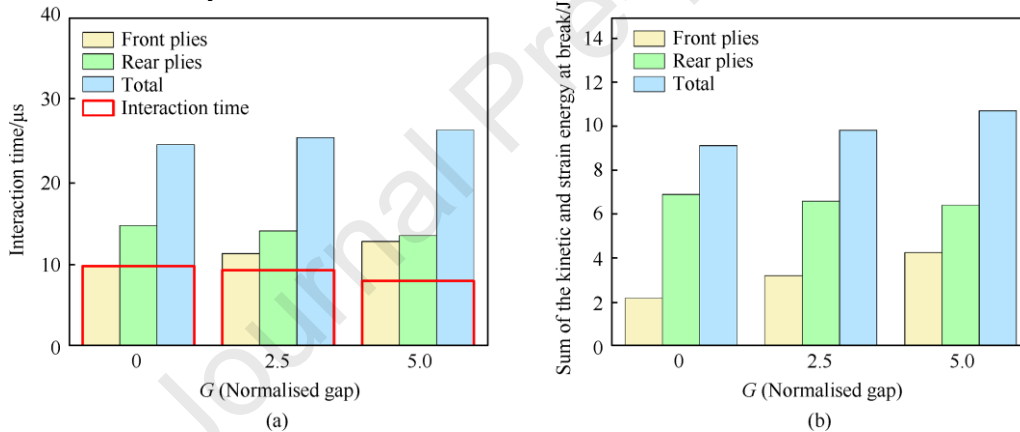


Fig. 8. The responses of the front and rear plies in "1+1" systems: (a) Projectile-fabric engagement time; (b) The sum of strain and kinetic energy at breakage.

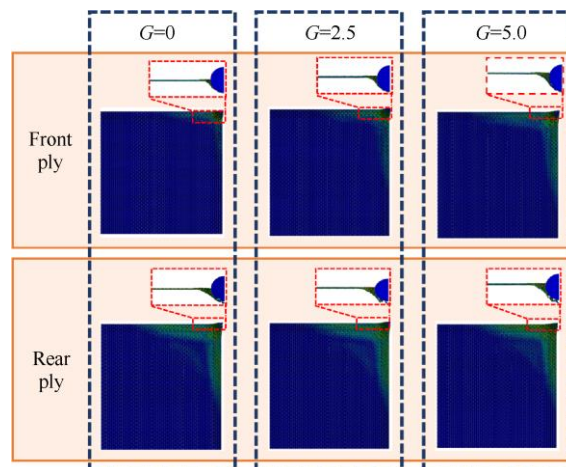


Fig. 9. Fabric deformation and stress distribution of the front and rear plies at the impact velocity of 400 m/s .

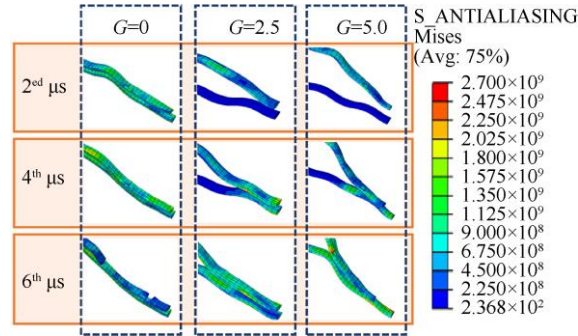


Fig. 10. Responses of the primary yarns at 2^{ed} μ s, 4th μ s and 6th μ s after impact.

5.2. The influence of system thickness

The numerical predictions shown in Fig. 7 indicate that the critical G for the “1+1”, “2+2” and “3+3” systems are approximately 3.75, 3, and 2. This subsection aims to resolve another problem: why the value of critical G decreases when the fabric system becomes thicker. It has been established in the previous section that the gap un-constrains the transverse deflection, releases stress concentration at the impact site, and prolongs the projectile-fabric engagement time. This consequently improves the energy absorption capability of the front ply. In terms of the “2+2” and “3+3” systems, the value of the critical G would be unchanged if the projectile-fabric engagement time doubles and triples. Nevertheless, it appears in Fig. 11(a) that the projectile-fabric engagement time of the front set of plies does not multiply with the number of plies. e.g., these values are 9.8 μ s (“1+1” system), 10.6 μ s (“2+2” system), and 11.8 μ s (“3+3” system) when $G=0$. The prolonged projectile-fabric engagement time in “2+2” and “3+3” systems reasonably require widened ply gaps to release the transverse deflection so that the potential of the front set of plies can be fully explored. The ply gaps should be greater than 1.5 mm ($G=3.75$ in the “1+1” system) but definitely smaller than 3 mm ($G=3.75$ in the “2+2” system) and 4.5 mm ($G=3.75$ in the “3+3” system). This is because the front plies in “2+2” and “3+3” systems fail earlier than expected and therefore do not need a 3 mm or 4.5 mm ply gap to minimize the interference between the front and rear sets of plies. Evidence can be found in Fig. 11(a), where there is limited interaction between the front and rear sets of ply when $G=5$. This causes that the amount of energy absorbed by the front and rear sets of ply appear to be similar in Fig. 11(b).

It is also found in Fig. 11(b) that the sum of the strain and kinetic energy accumulated on the panel at breakage increases approximately linearly with panel thickness. In terms of the front sets of plies, stress is distributed to a greater area on spaced systems (Fig. 12(a)); In terms of the rear sets of plies, the distribution of stress is shrinking as the ply gap increases in “2+2” systems (Fig. 12(b)), the phenomenon of which is less identifiable noticeable in “3+3” systems. This indicates that thicker systems respond more swiftly and more actively to energy dissipation than thinner systems when subjected to ballistic impact. In addition, the front set of plies is more sensitive to the ply gap than the rear set of plies, even in thicker systems.

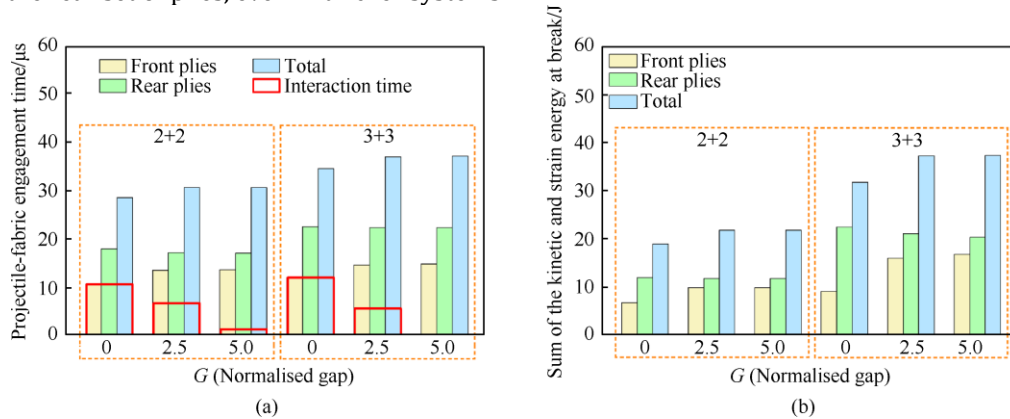


Fig. 11. The responses of the front and rear plies in “2+2” and “3+3” systems: (a) Projectiles-fabric engagement time; (b) The sum of strain and kinetic energy at breakage.

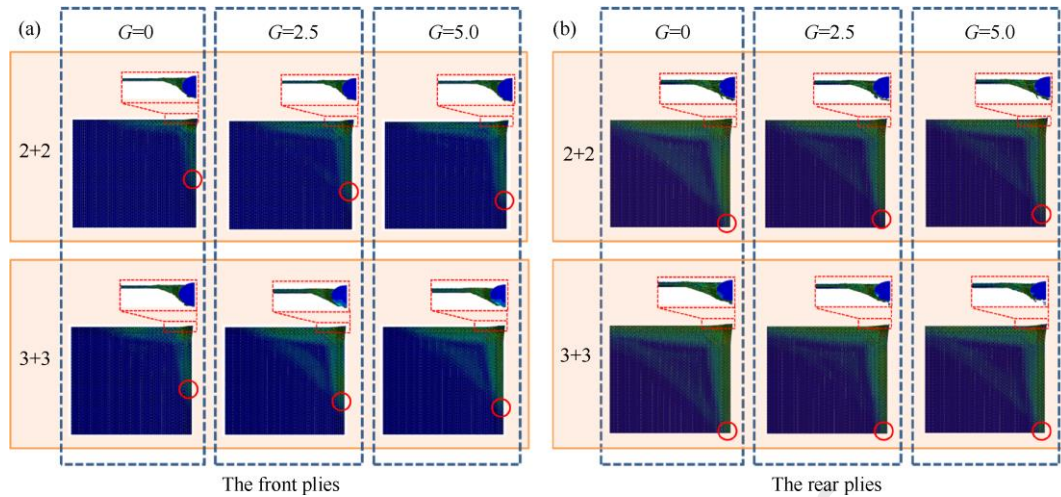


Fig. 12. Fabric deformation and stress distribution of the (a) front and (b) rear plies.

5.3. The influence of the impact velocity

The results and discussion shown above were based on the work undertaken at the impact velocity of 400 m/s. It is interesting to further study the responses of spaced systems at other impact velocities. Both experimental tests and FE simulations were performed over three impact velocities, i.e., 346 m/s (120 J), 283 m/s (80 J), and 200 m/s (40 J) to examine the role of impact velocity on the ballistic performance of the spaced system. The results shown in Fig. 13 suggested that the effect of the ply gap on the energy absorption of “1+1” systems diminishes as the impact velocity decreases. In terms of the experimental results, the improvement in energy absorption decreases from 34.4% (from $G=0$ to $G=5$) at the impact velocity of 400 m/s to 10.6% (from $G=0$ to $G=5$) at the impact velocity of 200 m/s. In terms of the numerical results, the improvement in energy absorption decreases from 23.6% (from $G=0$ to $G=5$) at the impact velocity of 400 m/s to 6.23% (from $G=0$ to $G=5$) at the impact velocity of 200 m/s. This is probably because that the duration of interaction between the front and rear plies increase dramatically at lower impact velocities (Fig. 14(a)).

In Fig. 15(a), the area of stress distribution and the transverse deflection on the front plies becomes increasingly greater as the impact velocity decreases and G increases. This is because the projectile-fabric engagement time is prolonged at low impact velocities and distanced ply gaps (Fig. 14(a)). Therefore, a greater amount of energy deposited on the front ply at breakage (Fig. 14(b)). What is interesting is that the deformation and stress distribution of the front ply are more sensitive to the gap at high impact velocities than those at low impact velocities, e.g., the energy variation from $G=0$ to $G=5$ is approximately 21.6% at 346 m/s, and this value is less than 5% at 200 m/s. This could probably be attributed to the fact that the stress concentration caused by the rear ply is more likely to cause failure on the front ply at high impact velocities than at low impact velocities; In terms of the rear ply, it is obvious that more material is involved in stress distribution as the impact velocity decreases. In addition, the rear ply is less sensitive to ply gap than the front ply at all the velocities (Fig. 15(b)). The ply gap appears to be less influential on the performance of the rear ply than the front ply, e.g., energy variation from $G=0$ to $G=5$ is less than 10% at 346 m/s (Fig. 14(b)). It was also found in Fig. 14(a) that the total projectile-fabric engagement time at 200 m/s are more than double and triple those at 283 m/s and 346 m/s, respectively. The amount of total energy accumulated at 200 m/s, however, is less than double those at 283 m/s and 346 m/s (Fig. 14(b)). This is probably because the kinetic energy of the projectile at 200 m/s (40 J) is considerably lower than 283 m/s (80 J) and 346 m/s (120 J). It follows that the efficiency of energy transmission from projectile to sample target is lower for the former case, and hence less amount of energy deposited on the fabric at breakage.

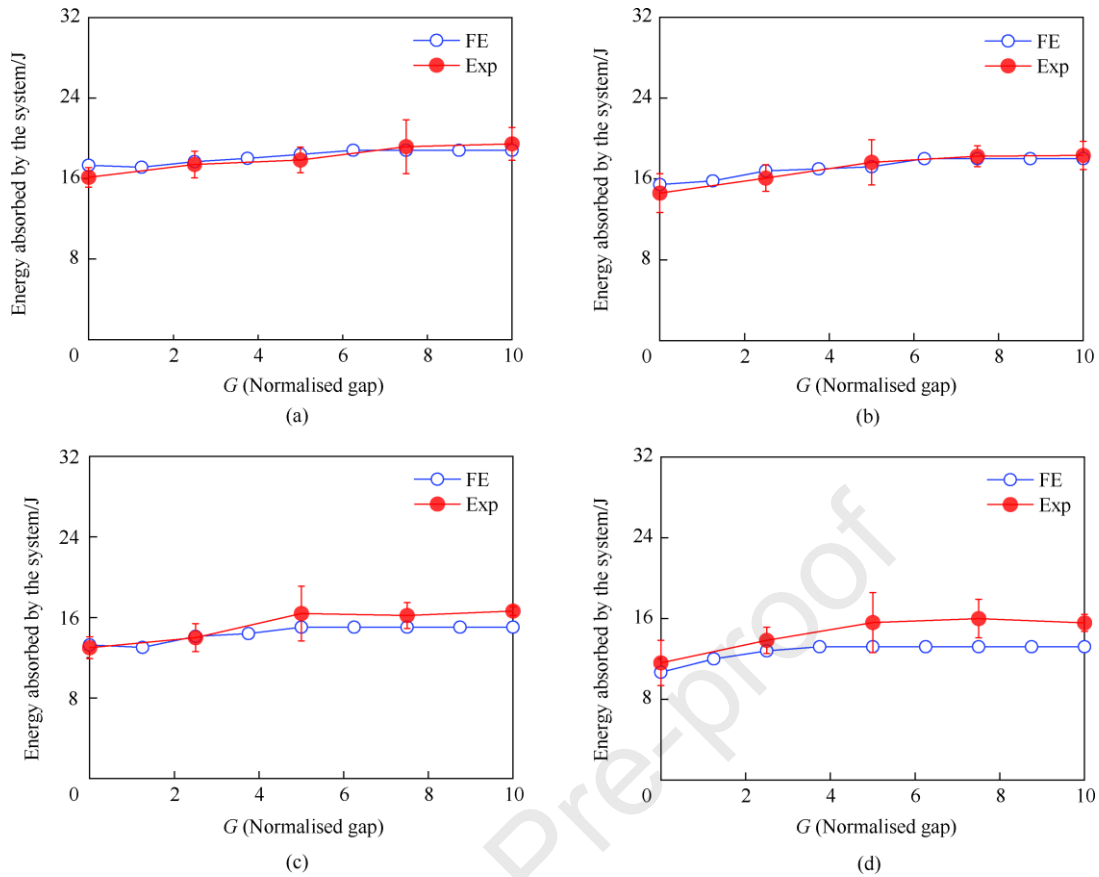


Fig. 13. Comparison of experimental and FE results of “1+1” systems at impact velocities of (a) 200 m/s; (b) 283 m/s; (c) 346 m/s; (d) 400 m/s.

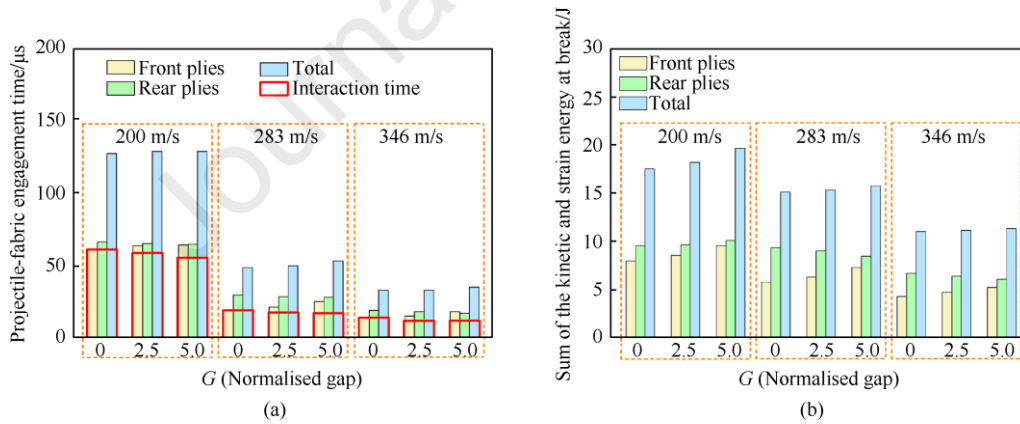


Fig. 14. The responses of the “1+1” systems at different impact velocities: (a) Projectile-fabric engagement time; (b) The sum of strain and kinetic energy at breakage.

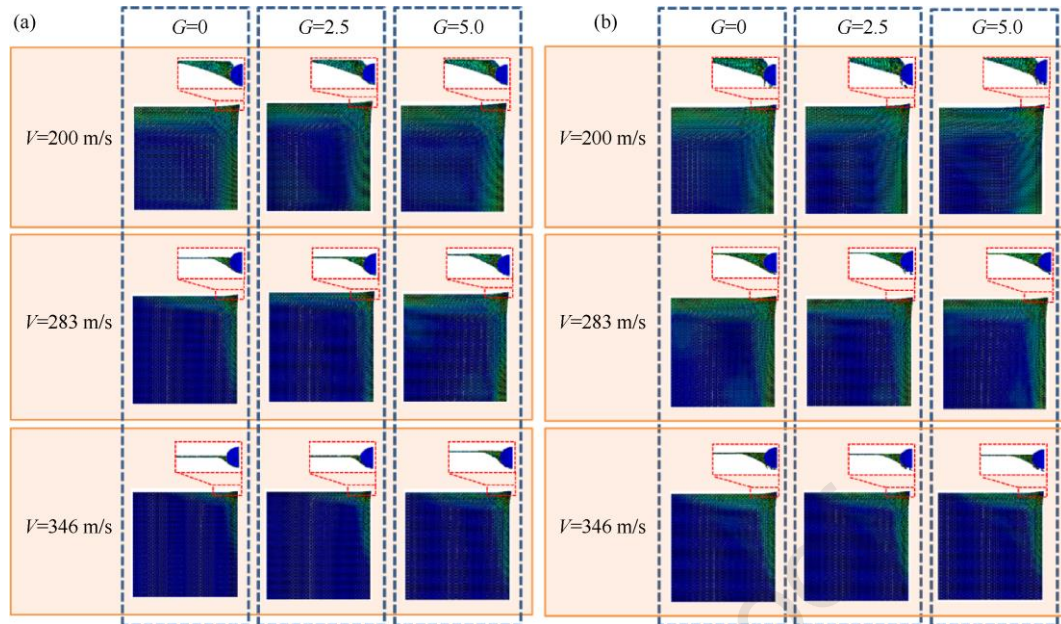


Fig. 15. Fabric deformation and stress distribution of the (a) front and (b) rear ply of the “1+1” systems at various impact velocities.

The numerical predictions displayed by the FE model suggested that the ballistic performance of a spaced multi-ply system is dependent on the effects of the ply gap and the impact velocity of the projectile. A greater ply gap shortens the interaction time between the front and rear set of plies, and a lower impact velocity weakens stress concentration at the impact site and delays the failure time of the front set of plies. These two factors combine to weaken the ply interference, during the process of which the response of the front and rear plies is assimilated and the energy absorption of the whole system is improved. Now, we can answer the question of why the value of critical G varies inversely with impact velocity in Fig. 13: when the impact velocity drops to 200 m/s, the engagement time between the projectile and the front ply is considerably prolonged, allowing a more defined transverse deflection. To obtain better ballistic performance, a wider ply gap is required to avoid interference between the front and rear sets of plies at low impact velocities.

5.4. The influence of the stacking order of the ply gap

Two types of panel were designed (Type A & Type B) to study the stacking order of the ply gap. Details of the panel were displayed in Table 3, and the energy absorption capability of Type A and B panels was shown in Fig. 16. The ballistic performance of spaced systems is dependent on the specific order in which the plies are stacked. The results suggested that placing a wider gap near the impact face and a narrow gap near the back face yields better performance than the reversed sequence. For “3+3” fabric systems, Type A4 absorbs 5.7% and 10.9% more energy than Type A3 and A2, respectively. During the penetration process in the multi-ply system, the projectile is progressively slowed. That means the projectile impacts the middle plies at a comparatively lower velocity than that impacts the front plies, and consequently, a wider gap is required for the former to accommodate sufficient energy absorption prior to material failure. In addition, systems with separated ply gaps exhibit greater energy absorption than those with combined ply gaps. For example, Type A4 and B4 exhibit around 11.6% and 19.8% increase in energy absorption when compared with their corresponding panel type of A5 and B6. This is probably because the former design has more free surfaces, and thus is more likely to explore the energy absorption potential of individual plies during the ballistic events than the latter.

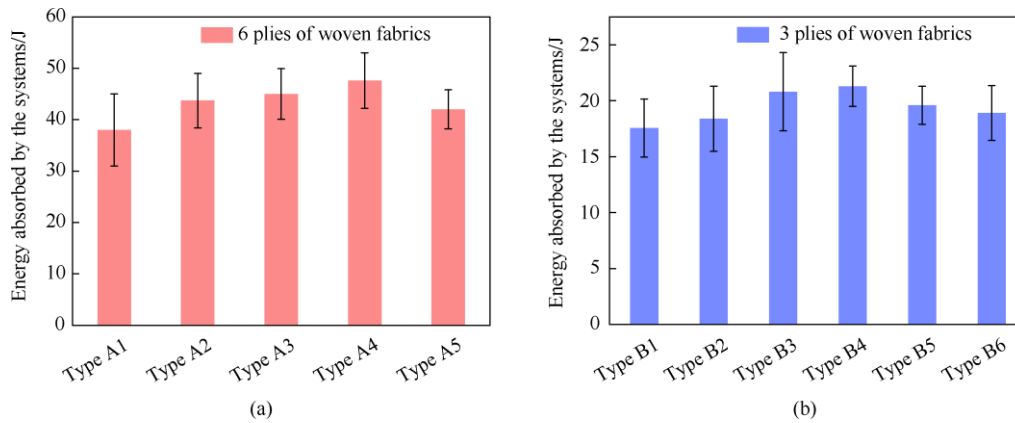


Fig. 16. Experimental results of (a) Type A and (b) Type B panels at an impact velocity of approximately 400 m/s.

6. Conclusions

The focus of this research was to examine the role of the ply gap on multi-ply fabric systems and develop guidelines for the engineering design of a lightweight flexible anti-ballistic system. The ballistic performance of spaced and non-spaced systems was characterized by using a gas gun and performing penetration tests. The fabric response under ballistic impact was predicted using FE simulation. It was found that the ballistic performance of the systems improves with a weakened ply interference, i.e., a reduction in interaction time between the front and rear sets of plies. This can be achieved by widening the ply gap. As the ply gap increases, the front set of plies tends to absorb more energy while the rear set absorbs less. The increment in the amount of energy absorbed by the former is sufficient to offset the reduction in the energy absorbed by the latter. When there is no interaction between the front and rear plies before the complete failure of the front plies, the whole system ceases to vary. In cases where the system becomes thicker and cases where the impact velocity becomes lower, a greater ply gap is required to accommodate the transverse deflection of the front plies so that the ballistic potential of spaced systems can be fully explored. The stacking order of the ply gap was also investigated, and the experimental results suggested a better energy absorption capability for spaced systems with a separated ply gap than for those with a combined ply gap or no gap.

Acknowledgments

This work was supported by the National Natural Science Foundation of China (Grant Nos. 51708553, 11502179), and Open Projects of State Key Laboratory for strength and vibration of mechanical structures (Grant No. SV2020-KF-17).

References

- [1] Zhou Y, Yao W, Zhang Z, Sun M, Xiong Z, Lin Y, Wang D, Wang M. The effect of cumulative damage on the ballistic performance of plain weaves. *Compos Struct* 2022, 297: 115978. <https://doi.org/10.1016/j.compstruct.2022.115978>.
- [2] Bajya M, Majumdar A, Butola BS, Arora S, Bhattacharjee D. Ballistic performance and failure modes of woven and unidirectional fabric based soft armour panels. *Compos Struct* 2021, 255:112941. <https://doi.org/10.1016/j.compstruct.2020.112941>.
- [3] Zhou Y, Ding S, Zhang Z, Li H, Lin Y, Sun M, Wang M. The Ballistic responses of thread-quilted plain weaves with increased yarn–yarn friction. *Thin Wall Struct* 2022, 171:108762. <https://doi.org/10.1016/j.tws.2021.108762>.
- [4] Bajya M, Majumdar A, Butola BS, Arora S, Verma SK, Bhattacharjee D. Design strategy for optimising weight and ballistic performance of soft body armour reinforced with shear thickening fluid. *Compos B Eng* 2020, 183:107721. <https://doi.org/10.1016/j.compositesb.2019.107721>.
- [5] Ignatova AV, Kudryavtsev OA, Zhikharev MV. Influence of surface polymer coating on ballistic impact response of multi-layered fabric composites: Experimental and numerical study. *Inter J Impact Eng* 2020, 144:103654. <https://doi.org/10.1016/j.ijimpeng.2020.103654>.
- [6] Ma Y, Dippolito M, Miao Y, Wang Y. A filament-level analysis on failure mechanism and ballistic limit of real-size multi-layer 2D woven fabrics under FSP impact. *Text Res J* 2021, 91(23-24): 2896-2910. <https://doi.org/10.1177/00405175211015518>.
- [7] Porwal PK, Phoenix SL. Modeling system effects in ballistic impact into multi-plyed fibrous

- materials for soft body armor. *Int J Fracture* 2005; 135(1):217-249. <https://doi.org/10.1007/s10704-005-3993-9>.
- [8] Wang Y, Chen X, Young R, Kinloch I, Wells G. A numerical study of ply orientation on ballistic impact resistance of multi-ply fabric panels. *Compos B Eng* 2015; 68:259-265. <https://doi.org/10.1016/j.compositesb.2014.08.049>.
- [9] Wang Y, Chen X, Young R, Kinloch I, Wells G. An experimental study of the effect of ply orientation on ballistic impact performance of multi-ply fabric panels. *Text Res J* 2016; 86(1):34-43. <https://doi.org/10.1177/0040517514566110>.
- [10] Liu JL, Singh AK, Lee HP, Tay TE, Tan VBC. The Response of Bio-inspired Helicoidal Laminates to Small Projectile Impact. *Inter J Impact Eng* 2020; 142(2020):103608. DOI:10.1016/j.ijimpeng.2020.103608.
- [11] Liu JL, Zhi J, Wong HL, Sugeng ES, Tay TE, Tan VBC. Effect of ply blocking on the high-speed impact performance of thin-ply CFRP laminates. *Compos Sci Technol*, 2022; 228(2022): 109640. DOI:10.1016/j.compscitech.2022.109640.
- [12] Arora S, Majumdar A, Butola BS. Soft armour design by angular stacking of shear thickening fluid impregnated high-performance fabrics for quasi-isotropic ballistic response. *Compos Struct* 2020; 233(1): 111720. <https://doi.org/10.1016/j.compstruct.2019.111720>.
- [13] Yuan Z, Wang K, Qiu J, Xu Y, Chen X. A numerical study on the mechanisms of Dyneema® quasi-isotropic woven panels under ballistic impact. *Compos Struct* 2020;236:111855. <https://doi.org/10.1016/j.compstruct.2020.111855>.
- [14] Karthikeyan K, Kazemahvazi S, Russell BP. Optimal fibre architecture of soft-matrix ballistic laminates. *Int J Impact Eng* 2016; 88:227-237. <https://doi.org/10.1016/j.ijimpeng.2015.10.012>.
- [15] Zhang G, Satapathy SS, Gonzalez V, Lionel R, Walsh SM. Ballistic impact response of Ultra-High-Molecular-Weight Polyethylene. *Compos Struct* 2015;133: 191-201. <https://doi.org/10.1016/j.compstruct.2015.06.081>.
- [16] Cunniff PM. An Analysis of the System Effects in Woven Fabrics under Ballistic Impact. *Text Res J* 1992; 62(9):495-509. <https://doi.org/10.1177/004051759206200902>.
- [17] Zhou Y, Gong X, Zhang Y, Xu C. A Numerical Investigation into the Influence of Ply Space on Panel Ballistic Performance. *Fiber Polym* 2015;16(12):2663-2669. <https://doi.org/10.1007/s12221-015-5662-6>.
- [18] Chen X, Zhou Y, Garry W. Numerical and Experimental Investigations into Ballistic Performance of Hybrid Fabric Panels. *Compos B Eng* 2014;58:35-42. <https://doi.org/10.1016/j.compositesb.2013.10.019>.
- [19] Porwal P, Phoenix S. Effects of layer stacking order on the V 50 velocity of a two-ply hybrid armor system. *J Mech Mater Struct* 2008; 3(4):627-639. <https://doi.org/10.2140/jomms.2008.3.627>.
- [20] Zhou Y, Hou J, Gong X, Yang D. Hybrid panels from woven Kevlar® and Dyneema® fabrics against ballistic impact with wearing flexibility. *J Text I* 2017; 109(8):1-8. <https://doi.org/10.1080/00405000.2017.1398122>.
- [21] Lim CT, Tan VBC, Cheong CH. Perforation of high-strength double-ply fabric system by varying shaped projectiles. *Inter J Impact Eng* 2020; 27(6):577-591. [https://doi.org/10.1016/S0734-743X\(02\)00004-0](https://doi.org/10.1016/S0734-743X(02)00004-0).
- [22] Zhou Y, Li H, Zhang Z, Li G, Xiong M. Ballistic response of stitched woven fabrics with superior energy absorption capacity: Experimental and numerical investigation. *Compos Struct* 2020:113328. <https://doi.org/10.1016/j.compstruct.2020.113328>.
- [23] Yang Y, Chen X. Study of energy absorption and failure modes of constituent layers in body armour panels. *Compos B Eng* 2016;98:250-259. <https://doi.org/10.1016/j.compositesb.2016.04.071>.
- [24] Yang EC, Linforth S, Ngo T, Tran P. Hybrid-mesh modelling & validation of woven fabric subjected to medium velocity impact. *Int J Mech Sci* 2018;144:427-437. <https://doi.org/10.1016/j.ijmecsci.2018.05.017>.
- [25] Yang Y, Chen X. Investigation on energy absorption efficiency of each ply in ballistic armour panel for applications in hybrid design. *Compos Struct* 2017;164:1-9. <https://doi.org/10.1016/j.compstruct.2016.12.057>.
- [26] Zhou Y, Chen X, Wells G. Influence of yarn gripping on the ballistic performance of woven fabrics from ultra-high molecular weight polyethylene fibre. *Compos B Eng* 2014; 62: 198-204. <https://doi.org/10.1016/j.compositesb.2014.02.022>.
- [27] Emre P, Howie F. On a Multi-Scale Finite Element Model for Evaluating Ballistic Performance of

- Multi-Ply Woven Fabrics. *Compos Struct* 2019; 207:488-508. <https://doi.org/10.1016/j.compstruct.2018.09.080>.
- [28] Hillerborg A, Mod er M, Petersson P.-E. Analysis of Crack Formation and Crack Growth in Concrete by Means of Fracture Mechanics and Finite Elements. *Cem Concr Res* 1976; 6(6):773-781. [https://doi.org/10.1016/0008-8846\(76\)90007-7](https://doi.org/10.1016/0008-8846(76)90007-7).
- [29] Yang Y, Chen X. Influence of fabric architecture on energy absorption efficiency of soft armour panel under ballistic impact. *Compos Struct* 2019; 224:111015. <https://doi.org/10.1016/j.compstruct.2019.111015>.
- [30] Briscoe BJ, Motamedi F. Role of Interfacial Friction and Lubrication in Yarn and Fabric Mechanics. *Text Res J* 1990; 60: 697-708. <https://doi.org/10.1177/004051759006001201>.
- [31] Guo R, Chen N, Zheng J. A semi-empirical design parameter for determining the inelastic strike-face mass fraction of soft armor targets. *Int J Impact Eng* 2019;125:83-92. <https://doi.org/10.1016/j.ijimpeng.2018.10.007>.

Declaration of interests

The authors declare that they have no known competing financial interests or personal relationships that could have appeared to influence the work reported in this paper.

The authors declare the following financial interests/personal relationships which may be considered as potential competing interests:

Journal Pre-proof